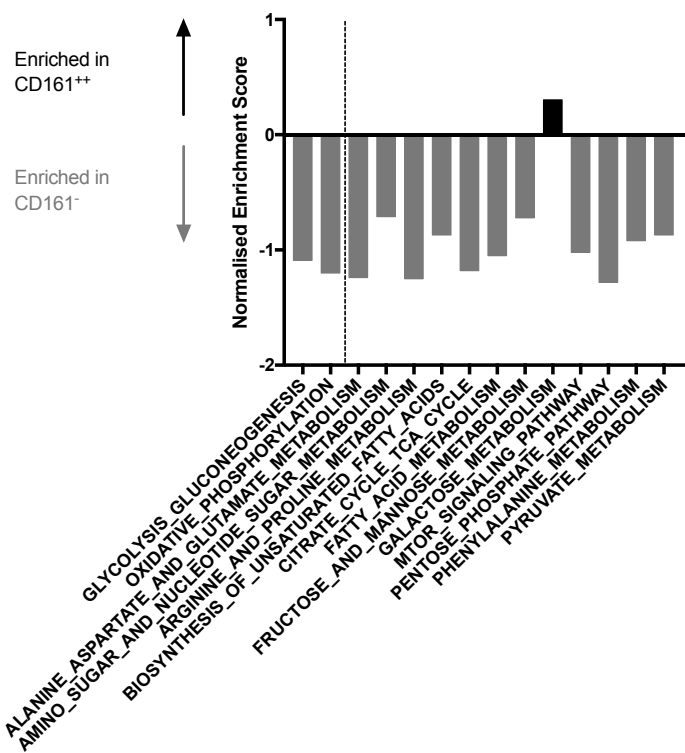
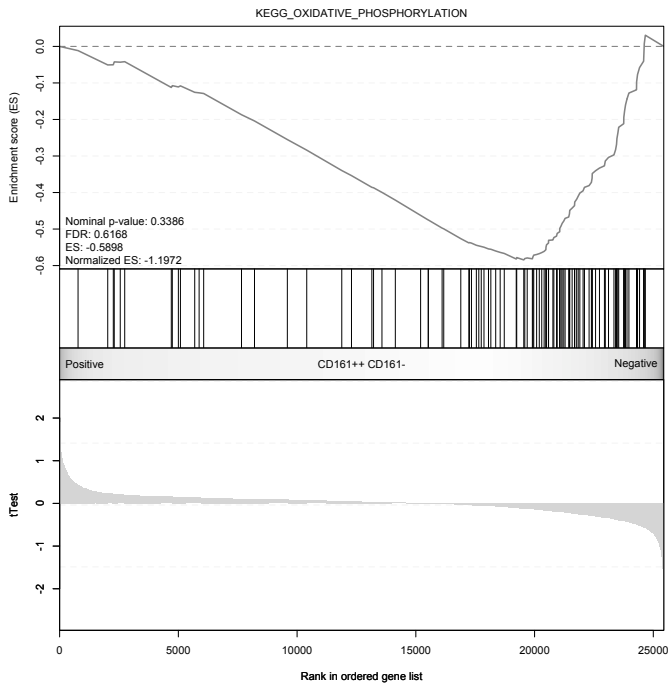


Supplementary Figure S1A



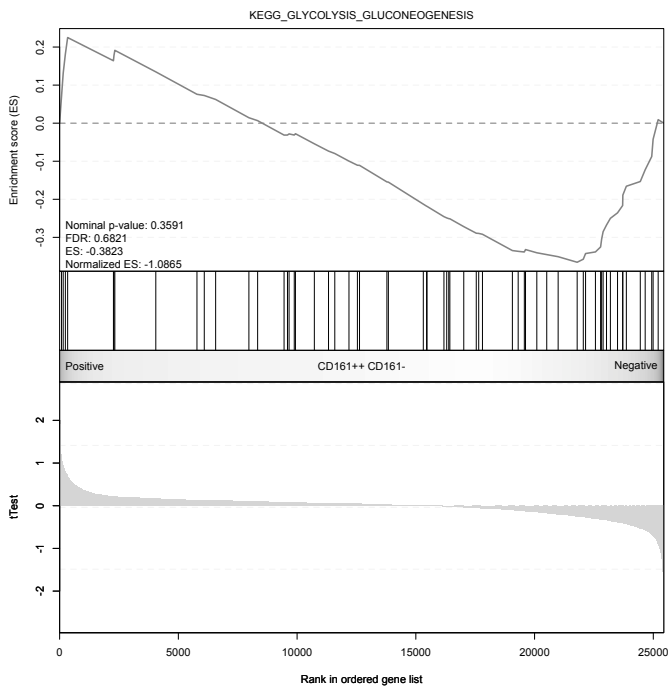
Supplementary Figure S1B

KEGG: OXPHOS



Supplementary Figure S1C

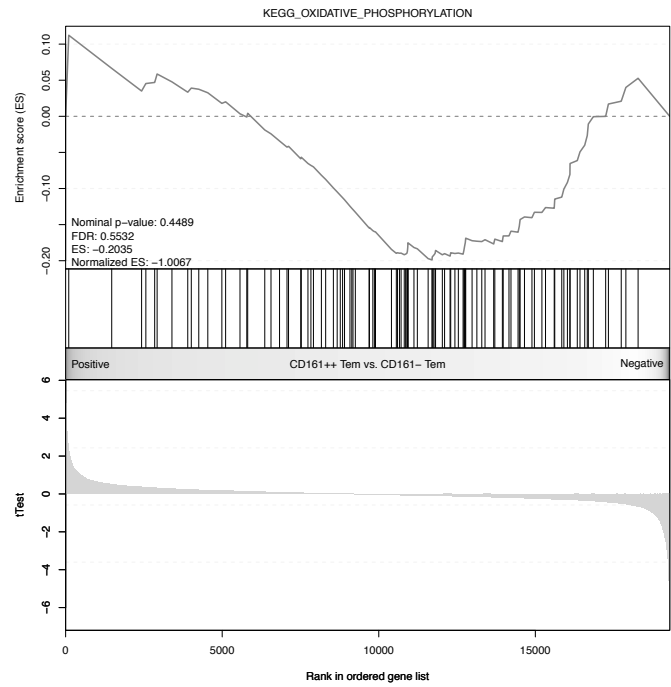
KEGG: Glycolysis



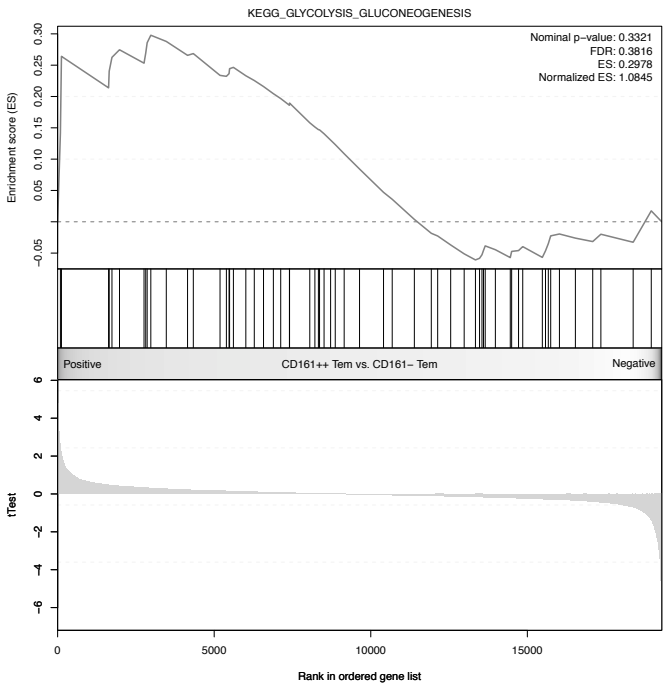
		SampleName	
ATPV0A1	ATPV0A1	ATPase, H+ transporting, lysosomal V0 subunit a1	
CXK1	CXK1	CoxII cytochrome c oxidase assembly homolog 15 (cerevisiae)	
ATPV0B	ATPV0B	ATPase, H+ transporting, lysosomal 21kDa, V0 subunit b	
ATPV0D1	ATPV0D1	ATPase, H+ transporting, lysosomal 38kDa, V0 subunit d1	
CXK6C	CXK6C	cytochrome c oxidase subunit 6c	
CXK7A1	CXK7A1	cytochrome c oxidase subunit VIIa polypeptide 1 (muscle)	
ATPV1G3	ATPV1G3	ATPase, H+ transporting, lysosomal 13kDa, V1 subunit G3	
CXK6E2	CXK6E2	cytochrome c oxidase subunit VIb polypeptide 2 (testis)	
ATPV0A4	ATPV0A4	ATPase, H+ transporting, lysosomal V0 subunit a4	
ATPA6P1	ATPA6P1	ATPase, H+ transporting, lysosomal accessory protein 1	
NDUFC2	NDUFC2	NAOH dehydrogenase (ubiquinolone) 1, subcomplex unknown, 2, 14,5kDa	
ATF4	ATF4	ATPase, H+/K+ exchanging, beta polypeptide	
CXK4I2	CXK4I2	cytochrome c oxidase subunit IV isoform 2 (lung)	
CXK6A2	CXK6A2	cytochrome c oxidase subunit VIA polypeptide 2	
CXK7B1	CXK7B1	cytochrome c oxidase subunit VIIb2	
NDUF5E	NDUF5E	NAOH dehydrogenase (ubiquinolone) Fe-S protein 6, 13kDa (NAOH-coenzyme 0 reductase)	
ATPV0C	ATPV0C	ATPase, H+ transporting, lysosomal 16kDa, V0 subunit c	
ATPV1C2	ATPV1C2	ATPase, H+ transporting, lysosomal 42kDa, V1 subunit C2	
NDUF87	NDUF87	NAOH dehydrogenase (ubiquinolone) i beta subcomplex, 7, 18kDa	
ATP12A	ATP12A	ATPase, H+/K+ transporting, nongastric, alpha polypeptide	
ATPV1A	ATPV1A	ATPase, H+ transporting, lysosomal 70kDa, V1 subunit A	
NDUF81	NDUF81	NAOH dehydrogenase (ubiquinolone) i beta subcomplex, 1, 7kDa	
ATPV1E1	ATPV1E1	ATPase, H+ transporting, lysosomal 31kDa, V1 subunit F1	
ATPV1B2	ATPV1B2	ATPase, H+ transporting, lysosomal 56/58kDa, V1 subunit B2	
ATPV1G2	ATPV1G2	ATPase, H+ transporting, lysosomal 13kDa, V1 subunit G2	
ATPV0D2	ATPV0D2	ATPase, H+ transporting, lysosomal 38kDa, V0 subunit d2	
NDUFV2	NDUFV2	NAOH dehydrogenase (ubiquinolone) flavoprotein 2, 24kDa	
ATPV1D	ATPV1D	ATPase, H+ transporting, lysosomal V0 subunit d	
ATPV0A2	ATPV0A2	ATPase, H+ transporting, lysosomal V0 subunit a2	
ATPSG3	ATPSG3	ATP synthase, H+ transporting, mitochondrial F0 complex, subunit c3 (subunit 9)	
NDUF5H	NDUF5H	NAOH dehydrogenase (ubiquinolone) Fe-S protein 1, 28kDa (NAOH-coenzyme 0 reductase)	
ATP4R	ATP4R	ATPase, H+/K+ exchanging, beta polypeptide	
NDUF84	NDUF84	NAOH dehydrogenase (ubiquinolone) i beta subcomplex, 4, 15kDa	
UCRC6	UCRC6	ubiquinol-cytochrome c reductase core protein 6	
ATPV1C1	ATPV1C1	ATPase, H+ transporting, lysosomal 42kDa, V1 subunit C1	
NDUFV1	NDUFV1	NAOH dehydrogenase (ubiquinolone) flavoprotein 1, 51kDa	
CXK8	CXK8	cytochrome c oxidase subunit 8a (ubiquitous)	
ATPSJ2	ATPSJ2	ATP synthase, H+ transporting, mitochondrial F0 complex, subunit F2	
NDUF82	NDUF82	NAOH dehydrogenase (ubiquinolone) i beta subcomplex, 2, 8kDa	
CYC1	CYC1	cytochrome c1	
ATPV1B1	ATPV1B1	ATPase, H+ transporting, lysosomal 56/58kDa, V1 subunit B1 (Renal tubular acidosis with deafness)	
NDUFA3	NDUFA3	NAOH dehydrogenase (ubiquinolone) i alpha subcomplex, 3, 1kDa	
NDUFA11	NDUFA11	NAOH dehydrogenase (ubiquinolone) i alpha subcomplex, 11, 17kDa	
SDBH	SDBH	succinate dehydrogenase complex, subunit B, integral membrane protein	
ATPSF	ATPSF	ATP synthase, H+ transporting, mitochondrial F1 complex, epsilon subunit	
ATP51	ATP51	ATP synthase, H+ transporting, mitochondrial F0 complex, subunit E	
LOC64310	LOC64310	-	
NDUFA81	NDUFA81	NAOH dehydrogenase (ubiquinolone) i, alpha/beta subcomplex, 1, 8kDa	
NDUF810	NDUF810	NAOH dehydrogenase (ubiquinolone) i beta subcomplex, 10, 22kDa	
CXK7E	CXK7E	cytochrome c oxidase subunit VIIe	
NDUFA4	NDUFA4	NAOH dehydrogenase (ubiquinolone) i alpha subcomplex, 4, 9kDa	
PPA2	PPA2	pyrophosphatase (inorganic) 2	
NDUF88	NDUF88	NAOH dehydrogenase (ubiquinolone) i beta subcomplex, 8, 19kDa	
CXK6A1	CXK6A1	cytochrome c oxidase subunit VIA polypeptide 1	
LHP	LHP	-	
NDUFA1	NDUFA1	NAOH dehydrogenase (ubiquinolone) i alpha subcomplex, 1, 7.5kDa	
CXK6C	CXK6C	cytochrome c oxidase subunit VIC	
ATPV0E1	ATPV0E1	ATPase, H+ transporting, lysosomal 9kDa, V0 subunit e1	
NDUF5S	NDUF5S	NAOH dehydrogenase (ubiquinolone) Fe-S protein 8, 23kDa (NAOH-coenzyme 0 reductase)	
NDUF6E	NDUF6E	NAOH dehydrogenase (ubiquinolone) i beta subcomplex, 6, 17kDa	
CXK5A	CXK5A	cytochrome c oxidase subunit Va	
ATPSG1	ATPSG1	ATP synthase, H+ transporting, mitochondrial F0 complex, subunit C1 (subunit 9)	
NDUF7	NDUF7	NAOH dehydrogenase (ubiquinolone) i alpha subcomplex, 7, 14.5kDa	
NDUFA9	NDUFA9	NAOH dehydrogenase (ubiquinolone) i alpha subcomplex, 9, 39kDa	
ATPSF1	ATPSF1	ATP synthase, H+ transporting, mitochondrial F0 complex, subunit B1	
ATP5B	ATP5B	ATP synthase, H+ transporting, mitochondrial F1 complex, beta polypeptide	
ATPSA1	ATPSA1	ATP synthase, H+ transporting, mitochondrial F1 complex, alpha subunit 1, cardiac muscle	
CXK4I1	CXK4I1	cytochrome c oxidase subunit IV isoform 1	
NDUF53	NDUF53	NAOH dehydrogenase (ubiquinolone) Fe-S protein 3, 30kDa (NAOH-coenzyme 0 reductase)	
ATPD5	ATPD5	ATP synthase, H+ transporting, mitochondrial F1 complex, delta subunit	
CXK7A2	CXK7A2	cytochrome c oxidase subunit VIIa polypeptide 2 (liver)	
NDUF48	NDUF48	NAOH dehydrogenase (ubiquinolone) i alpha subcomplex, 8, 19kDa	
ATPSL	ATPSL	ATP synthase, H+ transporting, mitochondrial F0 complex, subunit G	
NDUF4S	NDUF4S	NAOH dehydrogenase (ubiquinolone) i alpha subcomplex, 5, 13kDa	
ATPF51	ATPF51	ATPase, H+ transporting, mitochondrial F0 complex, subunit F6	
ITCRG1	ITCRG1	T-cell, immune regulator 1, ATPase, H+ transporting, lysosomal V0 subunit A3	
ATPSG2	ATPSG2	ATP synthase, H+ transporting, mitochondrial F0 complex, subunit C2 (subunit 9)	
CXK7C	CXK7C	cytochrome c oxidase subunit VIIc	
NDU			

CD161^{hi} T_{EM} vs. CD161^{lo} T_{EM}

KEGG: OXPHOS

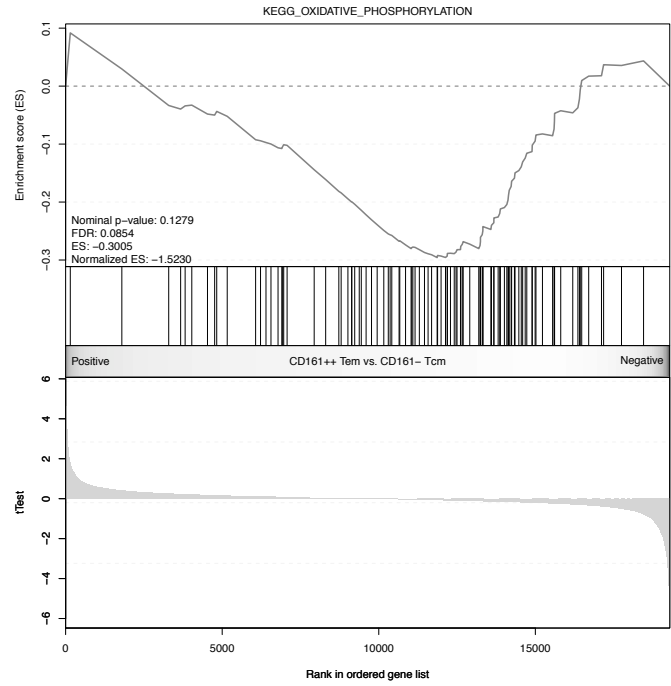


KEGG: Glycolysis

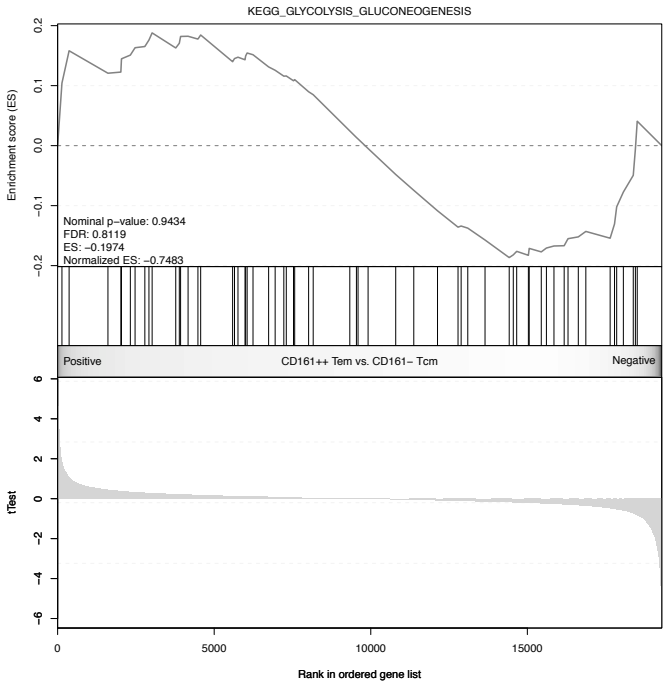


CD161^{hi} T_{EM} vs. CD161^{lo} T_{CM}

KEGG: OXPHOS

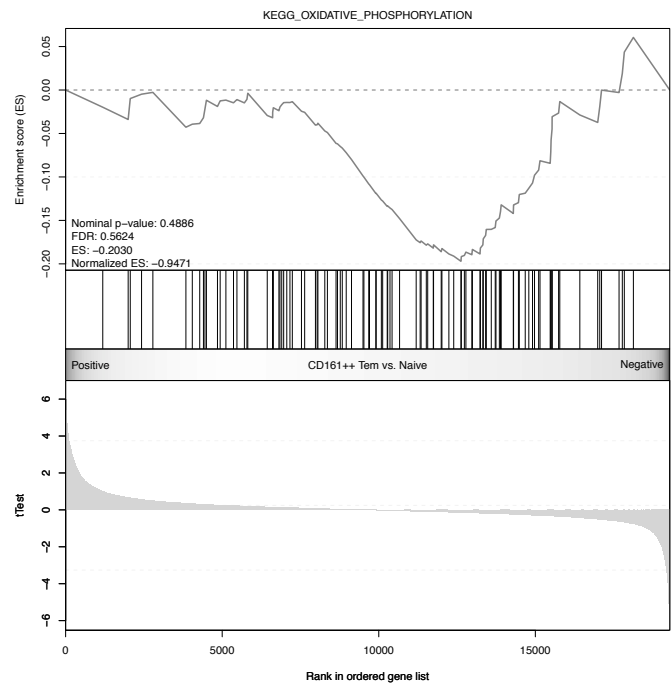


KEGG: Glycolysis

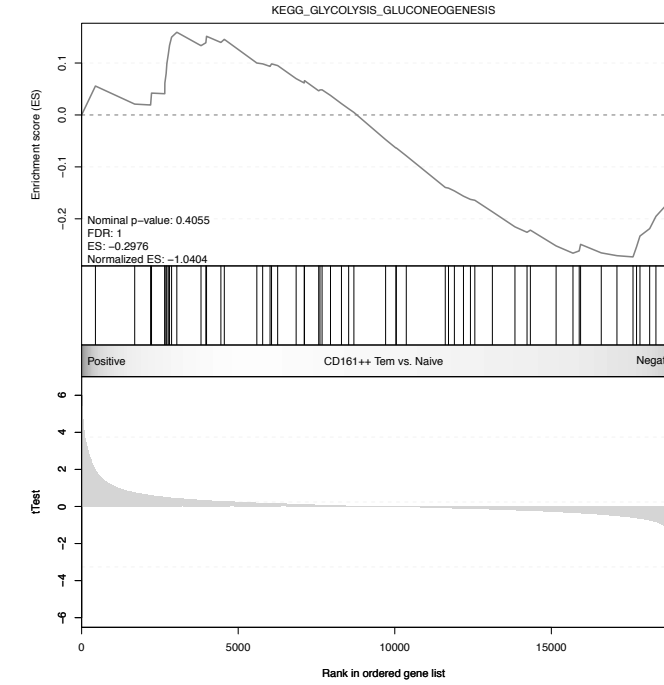


CD161^{hi} T_{EM} vs. T_N

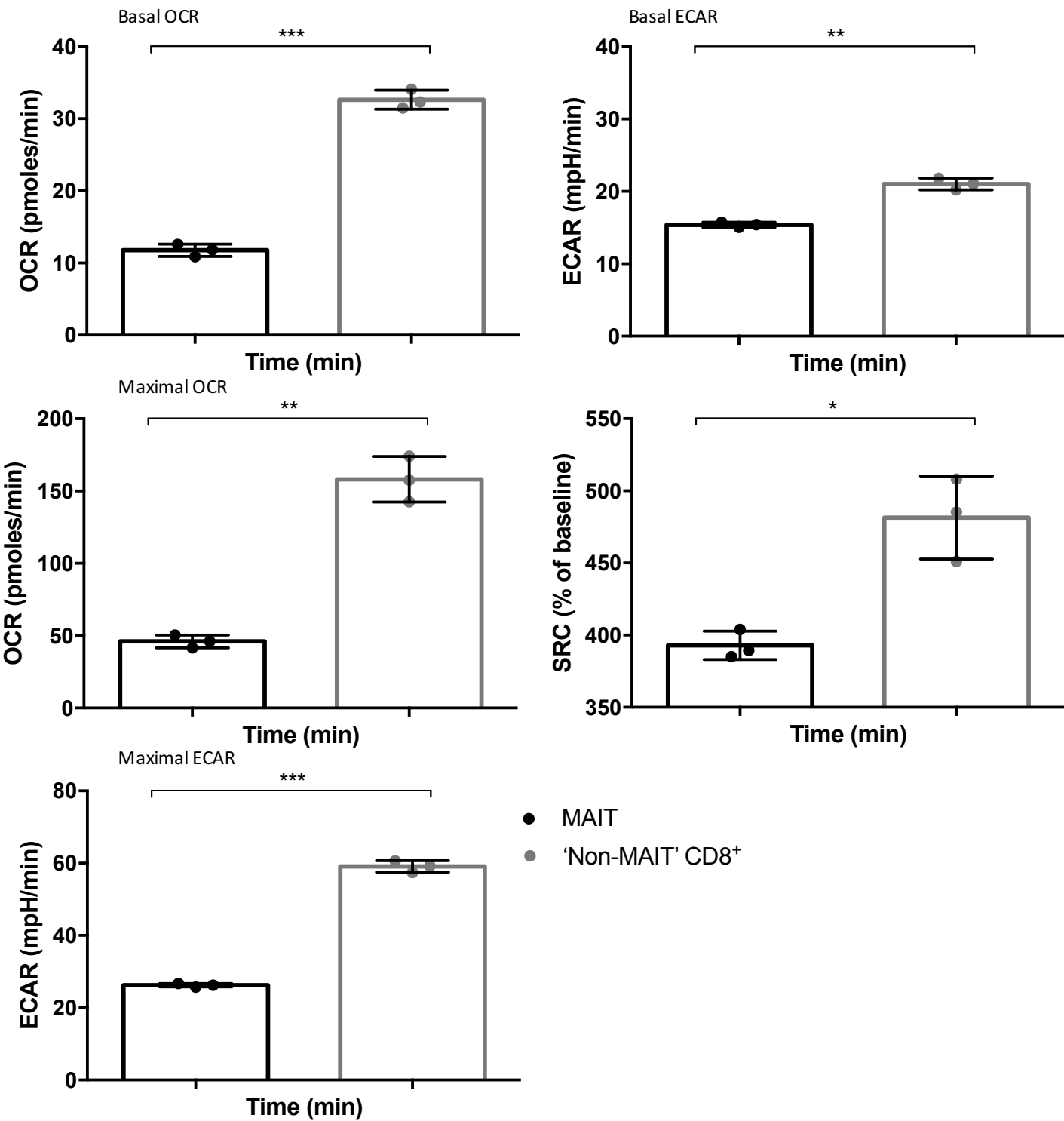
KEGG: OXPHOS



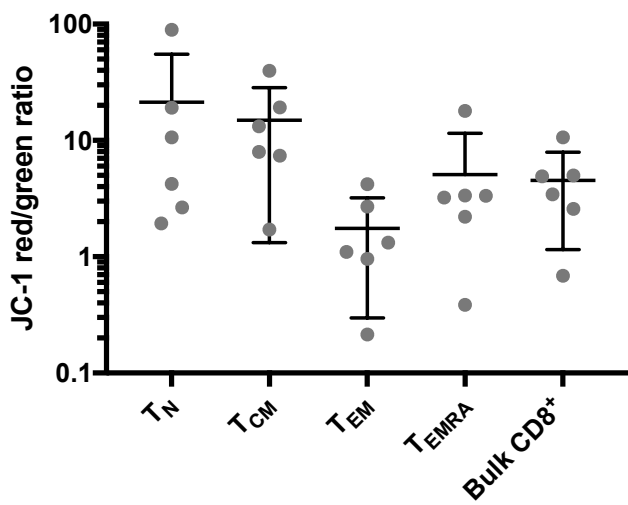
KEGG: Glycolysis



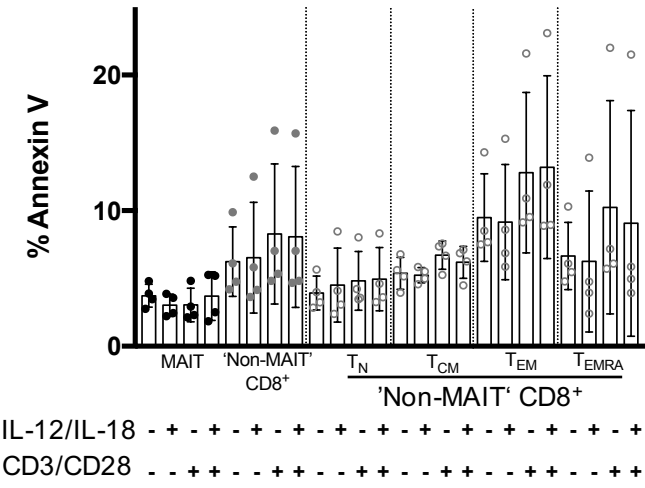
Supplementary Figure S2A



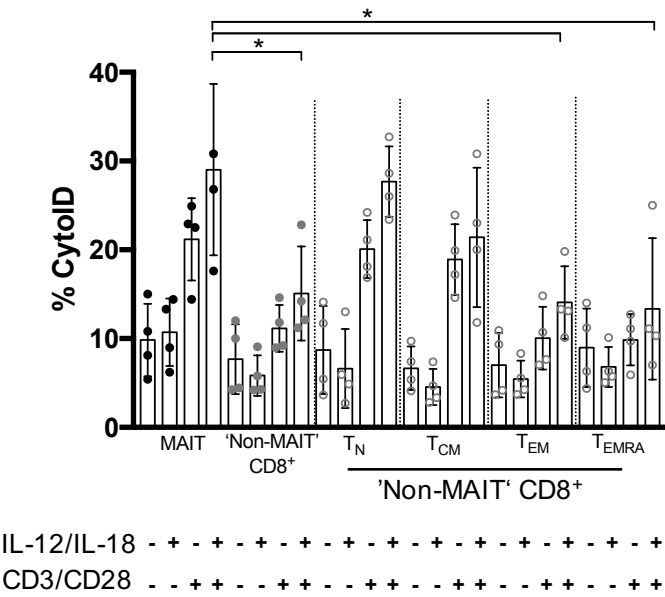
Supplementary Figure S2B



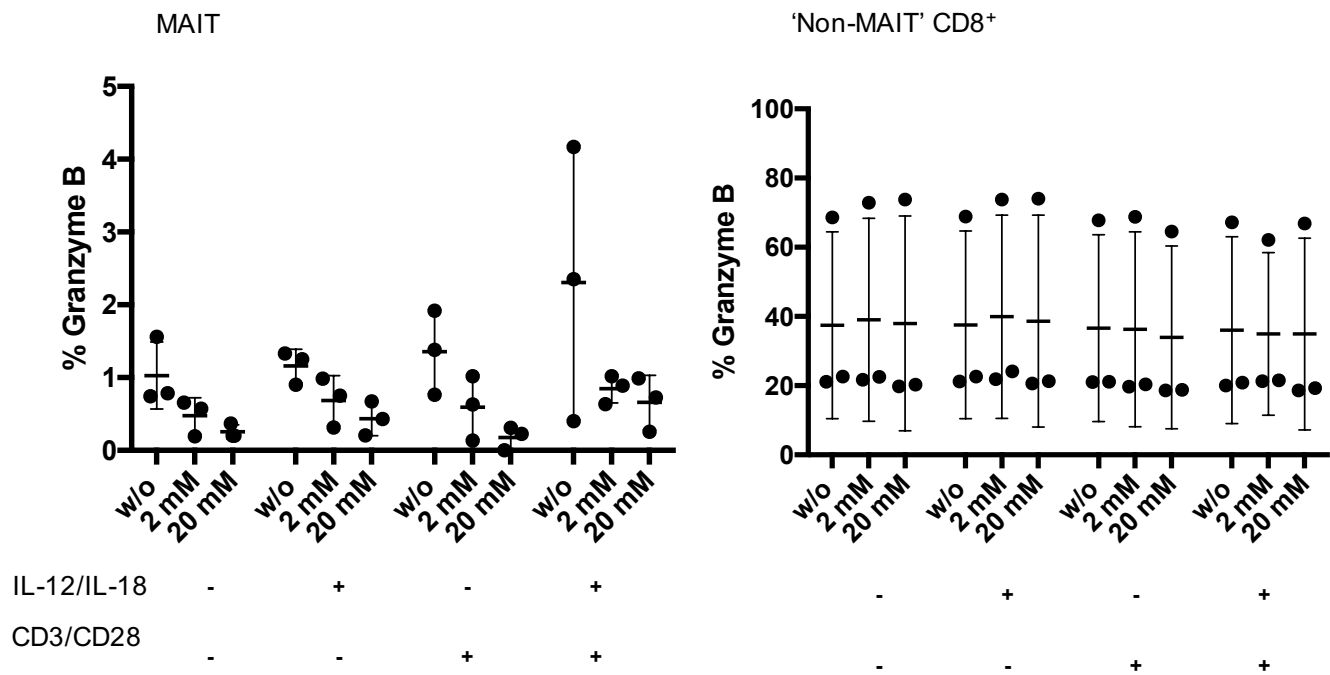
Supplementary Figure S2C



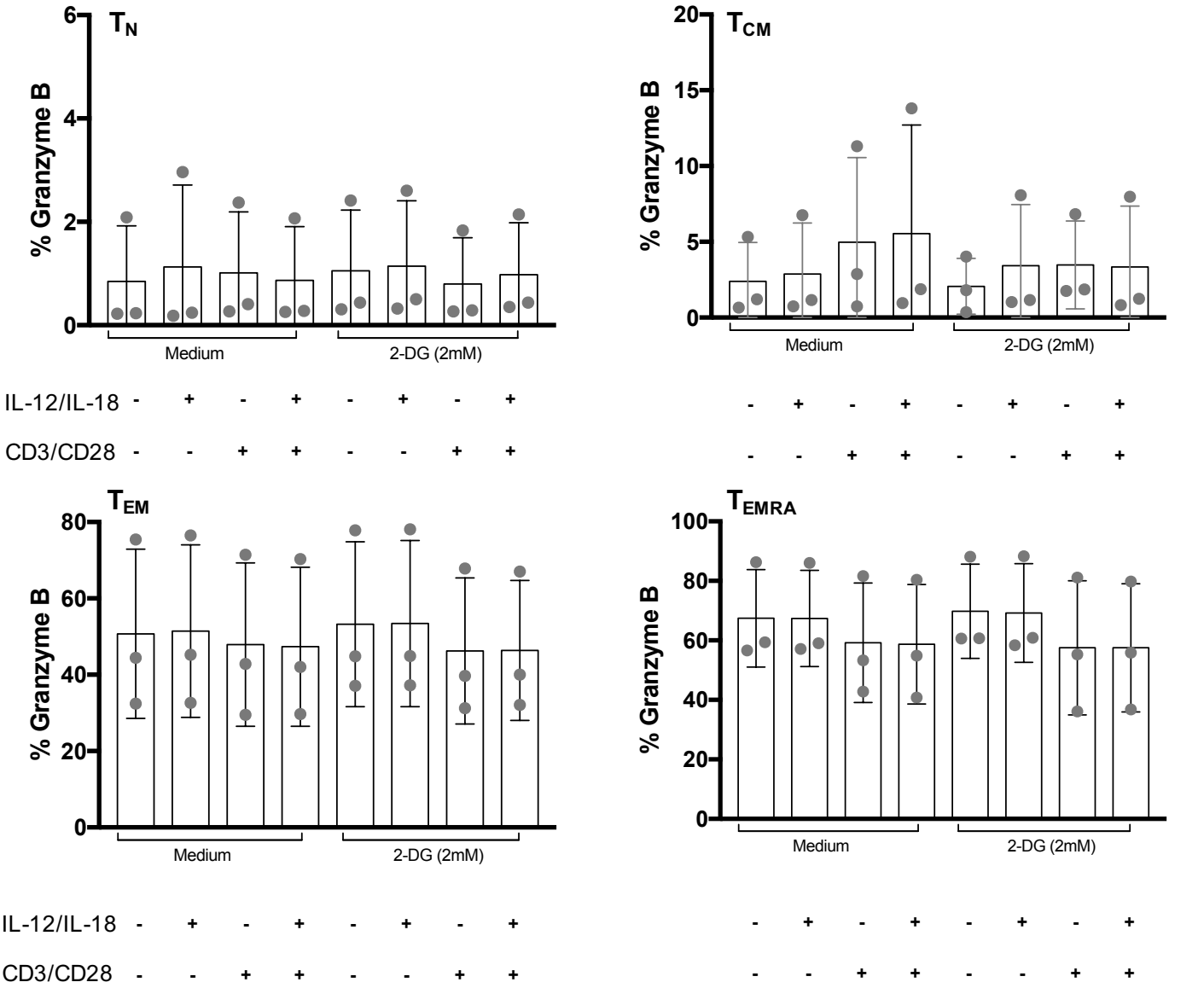
Supplementary Figure S2D



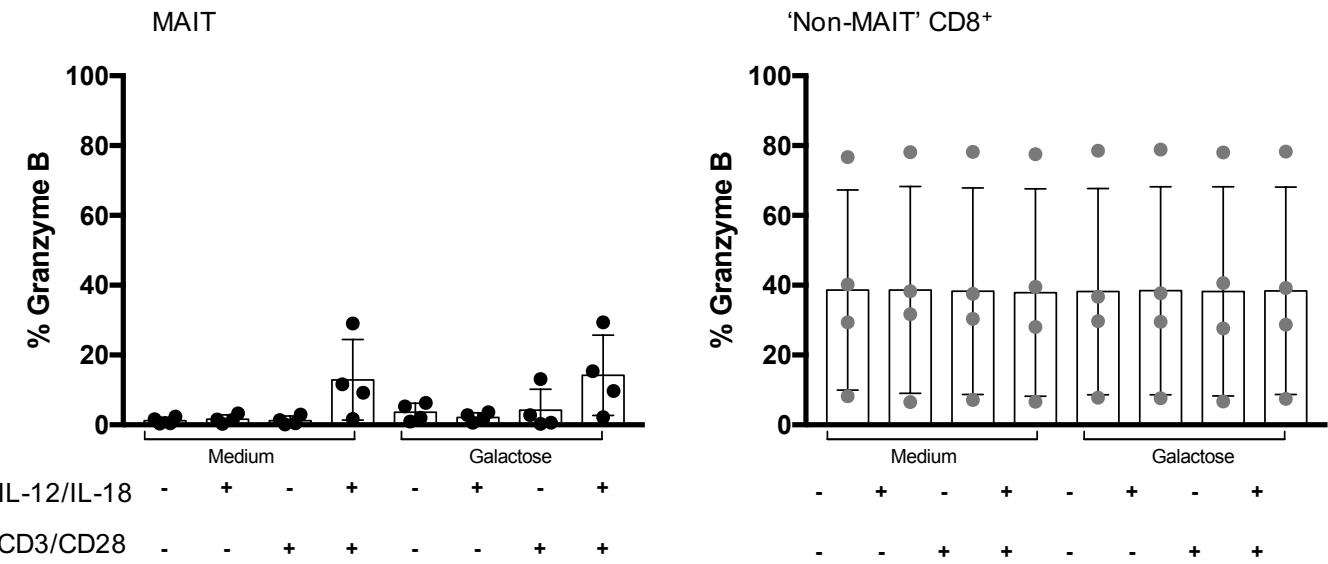
Supplementary Figure S3A



Supplementary Figure S3B



Supplementary Figure S3C



Supplementary Figure Legends

Supplementary Figure S1.

- (A)** Normalized enrichment scores (NES) for different metabolic gene sets comparing enrichment in CD161⁺⁺ CD8⁺ T cells (black) to CD161⁻ CD8⁺ T cells (grey) based on microarray profiling of CD161⁺⁺ CD8⁺ T cells or CD161⁻ CD8⁺ T cells. For the transcriptional analysis, sorted CD8⁺ T cells were used from four healthy donors.
- (B)** Enrichment plot of KEGG pathway for oxidative phosphorylation (OXPHOS) comparing CD161⁺⁺ (left) to CD161⁻ (right). Negative normalized enrichment score (NES) indicates negative enrichment in CD161⁺⁺ CD8⁺ T cells (NES=-1.1972).
- (C)** Enrichment plot of KEGG pathway for glycolysis and gluconeogenesis comparing CD161⁺⁺ (left) to CD161⁻ (right). Negative normalized enrichment score (NES) indicates negative enrichment in CD161⁺⁺ CD8⁺ T cells (NES=-1.0865).
- (D)** A heatmap of leading edge genes driving gene set enrichment of KEGG pathway of oxidative phosphorylation where the rank metric score of differential expression with the genes most upregulated in CD161⁺⁺ CD8⁺ T cells vs. CD161⁻ CD8⁺ T cells ranked on top of the list.
- (E)** Enrichment plot of KEGG pathway for oxidative phosphorylation (OXPHOS; left) and glycolysis (right) comparing CD161^{hi} T_{EM} to CD161^{lo} T_{EM} (upper panels). Enrichment plot of KEGG pathway for oxidative phosphorylation (left) and glycolysis (right) comparing CD161^{hi} T_{EM} to CD161^{lo} T_{CM} (middle panels). Positive normalized enrichment score (NES) indicates enrichment in CD161^{hi} T_{EM} CD8⁺ T cells. Lower panels show enrichment plots for oxidative phosphorylation (left) and glycolysis (right) comparing CD161^{hi} T_{EM} and naïve CD8⁺ T cells. Data from 6

healthy individuals are shown (GEO: GSE23663).

Supplementary Figure S2.

- (A)** Seahorse metabolic profiling was assayed on isolated MAIT cells and 'Non-MAIT' CD8⁺ T cells baseline oxygen consumption rate (OCR) and extracellular acidification rate (ECAR) were determined. Maximal OCR and spare respiratory capacity (SRC, expressed as the percentage of baseline) were measured upon injection of the mitochondrial uncoupling agent FCCP on the indicated cell types. Maximal ECAR was measured upon injection of oligomycin. Significance was determined using paired, parametric two-tailed t-test. Significance levels: * indicates $P < 0.05$, ** $P < 0.01$, *** $P < 0.001$. Error bars are a mean \pm SD. Data from two healthy donors in triplicate wells is shown.
- (B)** Measurement of mitochondrial polarization status using the ratiometric dye JC-1. Results are expressed as ratio of red/green fluorescence with a higher ratio indicating more polarized mitochondria. Examined cell types were T_N, T_{CM}, T_{EM} and T_{EMRA} and bulk 'Non-MAIT' CD8⁺ T cells. Data from six healthy donors is shown (representative of two independent experiments).
- (C)** Frequency of apoptotic cells measured by Annexin V staining of the indicated subsets: MAIT cells and 'Non-MAIT' CD8⁺ T cells (comprising T_N, T_{CM}, T_{EM} and T_{EMRA}) upon stimulation. Data is shown from n=4 healthy donors.
- (D)** Levels of autophagy measured by CytolD staining comparing MAIT cells and 'Non-MAIT' CD8⁺ T cells. Cells were either left untreated or stimulated with IL-12 and IL-18 (50 ng mL⁻¹) with or without stimulation with anti-CD3/CD28 beads as indicated. CD161⁺ cells comprise T_N, T_{CM}, T_{EM} and T_{EMRA}.

Significance was determined using paired, parametric two-tailed t-test. Significance levels: * indicates $P < 0.05$, ** $P < 0.01$, *** $P < 0.001$. Error bars show mean \pm SD. Data is shown from n=4 healthy donors (representative of two independent experiments).

Supplementary Figure S3.

(A) MAIT and 'Non-MAIT' CD8⁺ T cells were assayed for the intracellular expression of granzyme B in the presence or absence of the indicated stimuli (cytokines IL-12 and IL-18 (50 ng mL⁻¹) anti-CD3/CD28 stimulation) in the presence (2 mM or 20 mM) or absence of 2-deoxyglucose (w/o). Significance was determined using paired, parametric two-tailed t-test. Significance levels: * indicates $P < 0.05$, ** $P < 0.01$, *** $P < 0.001$. Error bars show mean \pm SD. Data is shown for n=3 healthy donors.

(B) 'Non-MAIT' CD8⁺ T cell subsets (T_N, T_{CM}, T_{EM} and T_{EMRA}) were assayed for the intracellular expression of granzyme B in the presence or absence of indicated stimuli (cytokines IL-12 and IL-18 (50 ng mL⁻¹) \pm anti-CD3/CD28 stimulation) in the presence or absence of 2-deoxyglucose (2 mM). Significance was determined using paired, parametric two-tailed t-test. Significance levels: * indicates $P < 0.05$, ** $P < 0.01$, *** $P < 0.001$. Error bars show mean \pm SD. Data is shown for n=3 healthy donors (representative of two independent experiments).

(C) MAIT and 'Non-MAIT' CD8⁺ T cells were assayed for the intracellular expression of granzyme B in the presence or absence of the indicated stimuli (cytokines IL-12 and IL-18 (50 ng mL⁻¹) \pm anti-CD3/CD28 stimulation) either in regular medium or in galactose supplemented medium (10 mM).

Significance was determined using paired, parametric two-tailed t-test. Significance levels: * indicates $P < 0.05$, ** $P < 0.01$, *** $P < 0.001$. Error bars show mean \pm SD. Data is shown from n=4 healthy donors (representative of two independent experiments).

Supplementary Methods

Gene Set Enrichment Analysis

For Gene Set Enrichment Analysis, we used gene sets from KEGG pathway gene lists (<http://www.genome.jp/kegg/pathway.html>). The obtained Normalized Enrichment Scores (NES) were used to compare KEGG pathways in CD161⁺⁺CD8⁺ T cells with CD161⁻CD8⁺ T cells. Furthermore, comparisons between CD161⁺⁺ CD8⁺ T cells and CD161⁻ T_N, T_{CM}, T_{EM} and T_{EMRA} CD8⁺ T cells were carried out using published microarray datasets on CD8⁺ memory subsets (T_N and T_{EMRA}) and CD161⁻ T_{CM} and T_{EM}¹.

Flow cytometry and ICS

For immunofluorescence staining, dead cells were excluded with the LIVE/DEADTM Fixable Near-IR Dead Cell Stain Kit (Life Technologies Ltd). Staining was performed with the following antibodies: anti-CD8 BV650, anti-Granzyme B AlexaFluor700 (BD Biosciences, Oxford, UK), anti-V α 7.2 PE or APC, anti-CD161 BV421, anti-CCR7 PerCP-Cy5.5, anti-CD69 FITC (BioLegend), anti-CD45RA PE-Cy7 (eBioscience, Life Technologies Ltd), anti-CD8 VioGreen (Miltenyi Biotec, Ltd.) and anti-CD27 FITC (BioLegend). Data were collected on a LSR II (BD Biosciences) and analyzed using FlowJo v.9.7.6 (BD Biosciences). In indicated experiments, staining for cellular markers was performed intracellularly using the Foxp3/Transcription Factor Staining Buffer Set (eBioscience, Life Technologies Ltd), according to the manufacturer's instructions.

Annexin V staining was used to assess frequencies of apoptotic cells using the APC Annexin V Apoptosis Detection Kit (BioLegend), according to the manufacturer's instructions after surface staining.

***In vitro* metabolic assays**

Mitochondrial polarization was additionally determined by JC-1 (Life Technologies Ltd) incubation (2 μ M) of labelled cells for 30 min at 37°C, 5% CO₂.

To assess mitochondrial ROS production, cells were first stained for surface markers and afterwards incubated with 5 μ M MitoSOX Red (Life Technologies Ltd) for 30 min at 37°C, according to the manufacturer's instructions and then acquired on a LSR II flow cytometer (BD Biosciences).

Measurement of autophagic vacuoles was performed using the CYTO-ID® Autophagy detection kit (Enzo Life Sciences, Exeter, UK), according to the manufacturer's instructions. Surface staining was performed after incubation with the fluorescent dye and fluorescence acquired by flow cytometry.

Seahorse Extracellular Flux Analysis

Triplicates of 330,000 cells per well of CD161⁺⁺V α 7.2⁺ CD8⁺ T cells and CD161⁻V α 7.2⁻ CD8⁺ T cells were plated on poly-D-lysine coated Seahorse XFp Cell Culture Miniplates, equilibrated for 30 min at 37°C. Before extracellular flux analysis, sorted cells were stimulated with 5 μ g mL⁻¹ plate bound anti-CD3 (OKT3, BioLegend) and 1 μ g mL⁻¹ soluble anti-CD28 (CD28.2, eBioscience, Life Technologies Ltd) for one hour at 37°C. For analysis of glycolytic capacity, cells were equilibrated in glucose-free medium according to the manufacturer's instructions. Cells were assayed for changes in oxidative consumption rate (OCR, pMoles/min) and extracellular acidification rate

(ECAR, mpH/min) after addition of oligomycin (1 μ M), FCCP (0.5 μ M) or antimycin A/Rotenone (0.5 μ M) for Mito Stress Test and after addition of glucose (10 mM), oligomycin (1 μ M) and 2-deoxyglucose (50 mM) for Glycolysis Stress Test.

Confocal Microscopy

For confocal microscopy, coverslips were coated with poly-D-lysine. After staining the cells on these coverslips, they were mounted onto microscope slides using VectaShield (Vector Laboratories Ltd., Peterborough, UK) and pictures acquired using a Zeiss LSM 880 Airyscan microscope, serial number 2802000323, (Helium-Neon Laser, 633 nm; GaAsP detector) using ZEN black software (Carl Zeiss Ltd, Oberkochen, Germany). Images were acquired at 16 bit. The pictures were processed using ImageJ v2.0.0 (www.imagej.net) without manipulation of threshold or signal ranges.

References

- 1 Turtle CJ, Delrow J, Joslyn RC *et al.* Innate signals overcome acquired TCR signaling pathway regulation and govern the fate of human CD161^{hi} CD8 α ⁺ semi-invariant T cells. *Blood* 2011; **118**: 2752–2762.